THE ASTROPHYSICAL JOURNAL, 376:430–438, 1991 August 1


# INFRARED AND VISIBLE PHOTOMETRY OF THE GRAVITATIONAL LENS SYSTEM 2237+030

DANIEL NADEAU[1]
Département de Physique, Université de Montréal, C.P. 6128, Succ. A, Montréal, QC, Canada, H3C 3J7, and Observatoire du Mont Mégantic
H. K. C. YEE[1]
Department of Astronomy, University of Toronto, Toronto, ON, Canada M5S 1A7
AND
W. J. FORREST,[1] J. D. GARNETT,[1] Z. NINKOV,[1,2] & J. L. PIPHER[1]
Department of Physics and Astronomy, University of Rochester, Rochester, NY 14627
*Received 1990 November 5; accepted 1991 January 29*

## ABSTRACT

As part of a program of high spatial resolution imaging of gravitationally lensed sources in the visible and infrared, images of 2237+030 were obtained in the Gunn $r$ and infrared $J$, $H$, $K$, and 3.3 $\mu$m filters. The results of the photometry of the four bright quasar components provide evidence of extinction through the lens and a determination of the extinction law in the galaxy is made. The energy distribution shows evidence of a sharp decrease of the spectral index $\alpha$ ($f_\nu \propto \nu^\alpha$) at wavelengths longer than a rest wavelength of 1 $\mu$m. Assuming that microlensing amplification in the infrared is of similar strength as in the visible, the data constrain the suggested microlensing event of 1988 August–September to a time scale of 100 days.

*Subject headings:* gravitational lenses — interstellar: grains — quasars

## 1. INTRODUCTION

The gravitational lens system 2237+030 was discovered as part of the Center for Astrophysics Redshift Survey (Huchra et al. 1985). A source with a quasar spectrum at redshift 1.695 was seen to be nearly coincident with the nucleus of this Zwicky galaxy of redshift 0.0394. This galaxy is an order of magnitude closer to us than any other lensing object yet discovered. Direct images in optical bands obtained at CFHT under $\sim 0''.7$ seeing by Yee (1988) clearly resolved the nuclear region of this system into four pointlike components surrounding the nucleus of the galaxy. Spatially resolved spectroscopic observation of the components by De Robertis & Yee (1988) and Filippenko (1989) demonstrated that the four components have nearly identical quasar line spectra at the same redshift, hence confirming the hypothesis that this is a gravitational lens system. Yee (1988) also showed that the four quasar components have different colors. Since gravitational lensing by itself is achromatic, Yee (1988) suggested that the components are affected by different amounts of reddening due to the different light paths through the lensing galaxy.

Models calculated by Schneider et al. (1988) and Kent & Falco (1988) could reproduce the positions and relative brightnesses of the quasar components reasonably well; the observed relative brightness of component C, however, is significantly higher than predicted by the models while that of component D is lower than predicted. Because of our proximity to the lensing galaxy, it has been suggested that microlensing events (i.e., temporary enhancement of one of the images due to gravitational lensing by a single starlike object crossing its light path) are likely to be observed in 2237+030 (Paczyński 1986; Kayser, Refsdal, & Stabell 1986; Kayser et al. 1987). If the "optical depth" of stars through the light path is sufficiently high, these events may explain the differences between the observed and calculated brightness values. Irwin et al. (1989) reported that such an event appeared to have made component A up to 0.5 mag brighter at the time of their observations than previously reported. Gravitational lensing in general is a probe of the total mass, dark and bright; microlensing may provide, in addition, a measure of the number densities of objects of different masses as the time scale of the event is a function of the mass of the microlens. Over time scales of months or years, microlensing probes mostly subsolar masses, of which very little is yet known. The maximum amplification factor during a microlensing event depends on the source size. Comparison of the amplification in the visible and in the infrared therefore could probe the size of the source as a function of wavelength. This information can be used to test the accretion disk models for quasars.

In this paper, the first images of 2237+030 obtained in the $J$, $H$, $K$, and 3.3 $\mu$m infrared bands are presented, as well as new images obtained in the visible. These data make it possible to determine the differential extinction affecting the different quasar components. Furthermore, because the observations were made near the time of those of Irwin et al. (1989), we were able to constrain the time scale of the proposed microlensing event observed by Irwin et al. (1989) to $\sim 100$ days.

The observations and method of data reduction are outlined in § 2. The observed energy distribution and evidence of selective extinction, aperture photometry of the galaxy, and the light curve of the brightness of component A with respect to component B, are presented in § 3. The implications of these results for the extinction law in the galaxy, and microlensing, are discussed in § 4, and a summary is given in § 5.

## 2. OBSERVATIONS AND DATA REDUCTION

Direct infrared images of 2237+030 were obtained at the Cassegrain f/36 focus of the CFHT 3.6 m telescope in the $J$, $H$, and $K$ bands on each of the nights of 1988 July 21, 22, and 24 (UT), and through a 3.3 $\mu$m filter on the nights of July 21 and

[1] Visiting Astronomer, Canada-France-Hawaii Telescope. The CFHT is operated by the National Research Council of Canada, the Centre National de la Recherche Scientifique of France, and the University of Hawaii.
[2] Postal address: Center for Imaging Science, Rochester Institute of Technology, Rochester, NY 14623.

TABLE 1

FLUX DENSITIES AT ZERO MAGNITUDE

| Band | $\lambda$ ($\mu$m) | $\Delta\lambda$ ($\mu$m) | log $\nu$ (Hz) | $f_\nu$(0 mag) (Jy) |
|---|---|---|---|---|
| $J$ ..... | 1.25 | 0.20 | 14.38 | 1638 |
| $H$ ..... | 1.65 | 0.32 | 14.26 | 1047 |
| $K$ ..... | 2.23 | 0.41 | 14.13 | 641 |
| 3.3 $\mu$m ..... | 3.255 | 0.23 | 13.96 | 331 |

24. The wavelength intervals and the flux calibrations of the infrared filters are given in Table 1. The flux calibrations are obtained from a curve fitted to data from Oke & Schild (1970), Gillett, Merrill, & Stein (1971), Gehrz, Hackwell, & Jones (1974), Blackwell et al. (1983), and Epchtein, Braz, & Sèvre (1984).

The infrared observations were made with the University of Rochester 62 × 58 InSb infrared camera (Forrest et al. 1989). The pixel pitch of the detector is 76 $\mu$m. The scale of the images was determined from double star measurements to be 0".295 ±0".001, 0".307±0".001, 0".304±0".001 pixel$^{-1}$ in the $J$, $H$, and $K$ bands respectively, in excellent agreement with the corresponding scales of 0".297±0".001, 0".310±0".002, and 0".304±0".001 pixel$^{-1}$ obtained by measurement of the distance separating the nucleus of the galaxy from a star located 8".69 to the NE, as determined from the visible data. This star is used as the reference point-spread function (PSF) in the subsequent analysis of the infrared quasar images. The infrared data were collected as sets of 42 s exposures on the source, interleaved at approximately 200 s intervals with similar exposures of a region of blank sky located 100" E of the object frames. Flat fields were obtained by observing the blue morning sky. A linearity correction function was determined from laboratory data obtained immediately after the observing run, and all the object, sky, and flat-field frames were corrected with this function. The maximum correction amounted to less than 0.2% for the object and sky frames, and less than 0.7% for the flat-fields.

Values interpolated from the two blank sky frames bracketing each object frame were subtracted from it, division by the flat-field was performed, and the bad pixels were replaced by an average over adjacent pixels (there were no bad pixels near the galaxy nucleus or the PSF). The resulting frames were examined and rejected if the image quality was degraded by the seeing or by guiding errors, or in a few cases by a temporary occurrence of a hot pixel near the source. The frames that were kept had a seeing of 0".7 to 0".8 FWHM.

The position of the source in the object frames was changed regularly during the observations over distances typical of the short-scale variations of the detector sensitivity. During data reduction the centroid of the emission from the galaxy nucleus and the quasar images was found for each frame, and the frames of a given night and wavelength band were shifted and co-added after expanding each original pixel into a box of 2 × 2 equal value pixels. This preserved some of the sampling information provided by the shifted frames. Because the source could not be detected in the individual images obtained through the 3.3 $\mu$m filter, the position of the source was not changed during these observations and a direct co-addition of the frames was performed. A journal of the infrared observations showing the integration times, the number of frames acquired and co-added, and the average seeing of the co-added images, is presented in Table 2. Figure 1 (Plate 7) shows the co-added $H$ band image obtained on 1988 July 21, and Figure 2 shows a contour plot of the sum of the co-added $H$ band images from all three nights.

Additional optical images were obtained, in Gunn $r$, $g$, and Johnson $B$ on 1988 November 12 UT, and in Gunn $r$ and Johnson $B$ on 1989 October 21 UT with the prime-focus direct camera at CFHT. The 1988 observations used the RCA4 detector, a 1024 × 640 CCD with pixel size of 15 $\mu$m and a scale of 0".206 pixel.$^{-1}$ The images were treated using biases and dome flats in the same manner as described in Yee (1988). Only the results from the $r$ images with integration times from 250 to 300 s will be presented in this paper. The seeing of the $r$ images varies from 0".55 to 0".65 FWHM. These optical images, along with the infrared data, effectively bracket the dates of observation of Irwin et al. (1989).

The analysis of the infrared images was performed on the data of each night separately. All the images were analyzed with the interactive image-processing package PPP (Yee 1991), using the iterative PSF subtraction procedure described in Yee (1988). A PSF was obtained for each co-added frame by first subtracting from the original frame a median-filter smoothed frame in which the star image had been replaced by interpolated values. This procedure is necessary because the PSF star is situated in the nebulosity of the lensing galaxy. The peak of the star image was found and the lower contours of this image were smoothed along arcs of 60° to 120° centered on the peak. This procedure reduced the effects of the noise in the

TABLE 2

JOURNAL OF INFRARED OBSERVATIONS

| Date (UT) | Filter | Integration Time per Frame (s) | Number of Frames Acquired | Number of Frames Co-added | Average Seeing |
|---|---|---|---|---|---|
| 1988 Jul 21..... | $J$ | 41.7 | 17 | 10 | 0".80 |
| | $H$ | 41.7 | 9 | 8 | 0.73 |
| | $K$ | 41.7 | 7 | 4 | 0.81 |
| | 3.3 $\mu$m | 1.67 | 40 | 40 | ... |
| 1988 Jul 22..... | $J$ | 41.7 | 8 | 5 | 0.74 |
| | $H$ | 41.7 | 16 | 11 | 0.82 |
| | $K$ | 41.7 | 18 | 11 | 0.73 |
| 1988 Jul 24..... | $J$ | 41.7 | 13 | 6 | 0.81 |
| | $H$ | 41.7 | 6 | 6 | 0.72 |
| | $K$ | 41.7 | 16 | 12 | 0.81 |
| | 3.3 $\mu$m | 1.67 | 40 | 40 | ... |

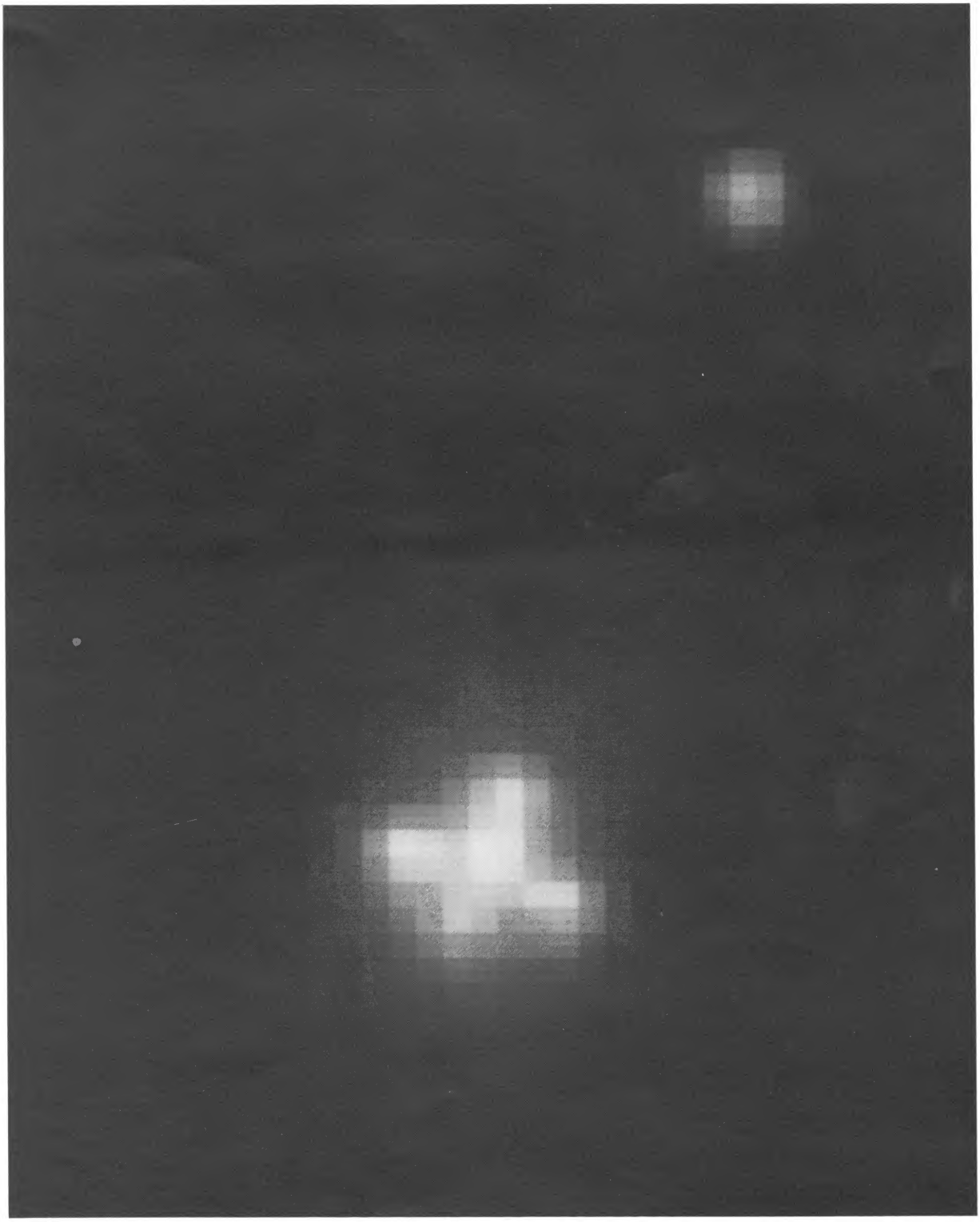

FIG. 1.—Image of the co-added data obtained in $H$ on 1988 July 21. North is up and East is to the left. As an indication of the scale, the distance between the southernmost component (A) and the northernmost component (B) is 1".8. The star used for the point spread function appears to the northeast.

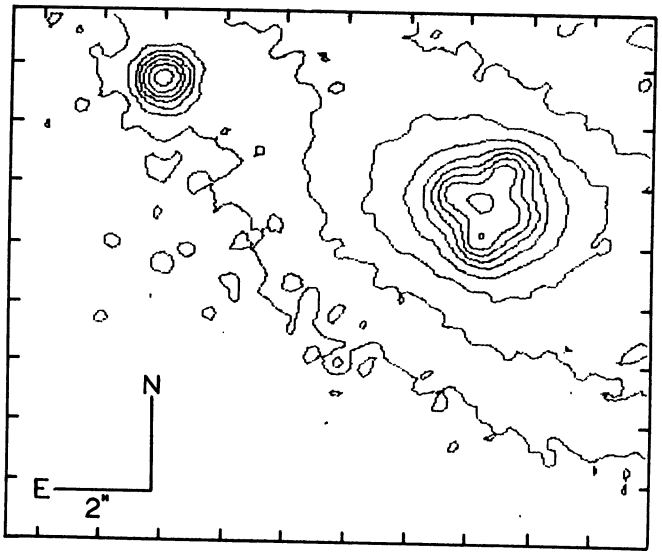


FIG. 2.—Contour plot of the sum of the *H* images obtained on 1988 July 21, 22, and 24, showing the galaxy, the four quasar components, and the PSF. The contours are a factor of 1.414 apart. Each tick mark represents 10 pixels, and the scale is 0".15 per pixel, half the scale of the original frames, as explained in the text. The image does not reproduce the entire original 62 × 58 frames because pixels at the edges of the frames were lost in the shift-and-add procedure.

PSF considerably while introducing negligible modifications of the radial and low-order azimuthal PSF profile. Once a first analysis of the infrared images had been done, the deduced contribution from the quasar components was removed and the position of the center of the galaxy was determined precisely. Using this position, the scale and orientation of the images, and the precise relative positions obtained by Yee (1988), improved positions were determined for the quasar components. The infrared images were re-analyzed using these positions, to obtain the final values of brightness ratios with respect to the PSF. The accuracy of the subtraction can be judged from the three night average images of the underlying galaxy shown in Figure 3. The average counts for zero magnitude (CFZM), obtained for each night from the data in Table 3, the integrated PSF signal, and the component to PSF brightness ratio, were used to obtain the magnitude of each component.

The uncertainty on the brightness ratio of components A and B has been determined by changing the ratio until a distinct asymmetry of the underlying galaxy could be seen. This generally required a change of 0.1 mag of the brightness ratio in the image from a single night. The uncertainties in the ratio of components C and D to component A are somewhat larger

TABLE 3

COUNTS FOR ZERO MAGNITUDE

| DATE (UT) | STAR | FILTER | | | |
|---|---|---|---|---|---|
| | | *J* | *H* | *K* | 3.3 μm |
| 1988 Jul 21..... | γ Lyr | 21,600 | 27,400 | 17,700 | ... |
| | κ And | 23,100 | 27,800 | 18,600 | ... |
| 1988 Jul 22..... | γ Lyr | ... | ... | 19,000 | 2980 |
| | σ Cyg | 22,500 | 28,500 | 17,500 | ... |
| | 4 Lac | 22,200 | 28,500 | 17,600 | 2789 |
| 1988 Jul 24..... | τ Her | ... | ... | 16,900 | ... |
| | 4 Lac | 21,600 | 26,400 | 16,600 | ... |
| | 4 Lac | 21,800 | 27,500 | 17,200 | ... |

because of the geometry of the source and the lower brightness of these components. The global uncertainty on the brightness of the four components was estimated by varying their brightness by a common factor.

## 3. RESULTS

### 3.1. *Energy Distribution of the Quasar Components*

Table 4 presents the magnitudes of the four quasar components as measured in the *J*, *H*, and *K* bands, as well as the differential magnitude of components *B*, *C*, and *D* with respect to component A. The uncertainty shown in Table 4 for the magnitude of component A includes the uncertainty on the integrated counts for this component and the uncertainty on the CFZMs, based on the reproducibility of the CFZM calibrations. No evidence of variation of the quasar components was found over the 4 day period of the observations, and the results presented are averages taken over the three observing nights.

The observed energy distribution of the quasar components is shown in Figure 4. The infrared fluxes are obtained from the data in Tables 1, 3, and 4. Visible magnitudes through Gunn *g*, *r*, and *i* filters are taken from Yee (1988). The transformation of the Gunn *g* and *r* magnitudes to multichannel spectrophotometer (MCSP) magnitudes is obtained from Yee (1983):

$$r_{\mathrm{MCSP}} = r_{\mathrm{Gunn}} - 0.15 + 0.06(g - r)_{\mathrm{Gunn}} ,$$

$$g_{\mathrm{MCSP}} = g_{\mathrm{Gunn}} + 0.05 + 0.07(g - r)_{\mathrm{Gunn}} ,$$

and the following approximate transformation of the Gunn *i* magnitude is used:

$$i_{\mathrm{MCSP}} \simeq i_{\mathrm{Gunn}} - 0.08 .$$

A flux of 3650 Jy corresponds to $\mathrm{mag}_{\mathrm{MCSP}} = 0$ (Gunn & Oke 1975; Oke & Schild 1970).

TABLE 4

INFRARED MAGNITUDES OF THE QUASAR COMPONENTS

| COMPONENT | MAGNITUDE | | | DIFFERENTIAL MAGNITUDE | | |
|---|---|---|---|---|---|---|
| | *J* | *H* | *K* | *J* | *H* | *K* |
| A ..... | 15.89 ± 0.08 | 15.26 ± 0.07 | 14.91 ± 0.08 | 0.0 | 0.0 | 0.0 |
| B ..... | 16.01 | 15.42 | 15.02 | 0.12 ± 0.06 | 0.17 ± 0.05 | 0.11 ± 0.06 |
| C ..... | 16.18 | 15.53 | 15.09 | 0.29 ± 0.08 | 0.27 ± 0.07 | 0.18 ± 0.08 |
| D ..... | 16.53 | 15.79 | 15.47 | 0.65 ± 0.10 | 0.54 ± 0.10 | 0.56 ± 0.10 |
| PSF ..... | 16.11 | 15.45 | 15.29 | ... | ... | ... |

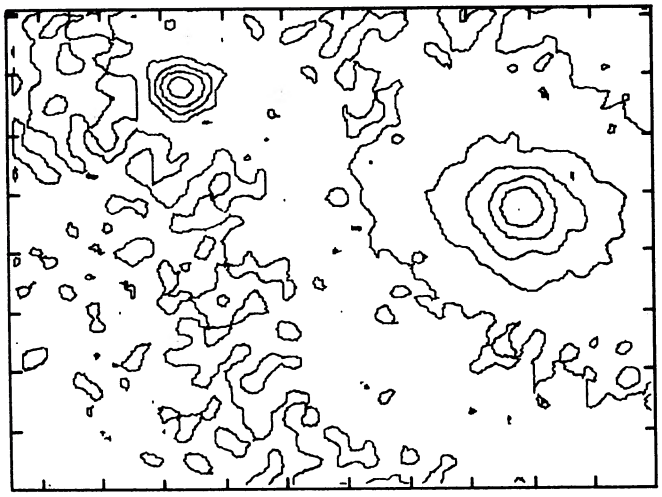

FIG. 3*a*

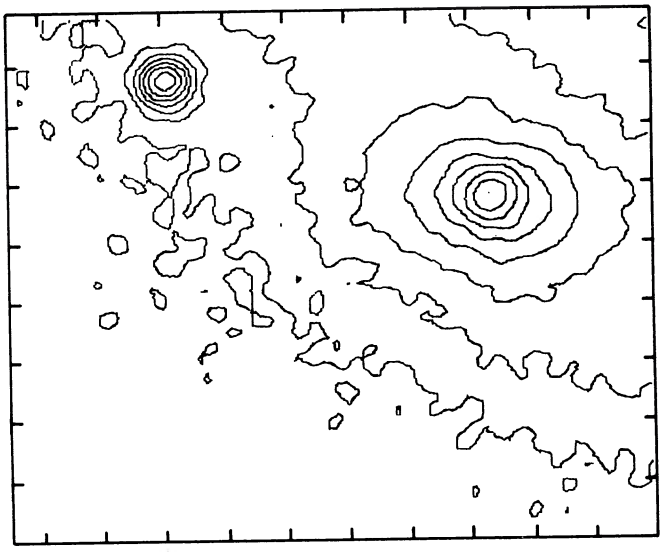

FIG. 3*b*

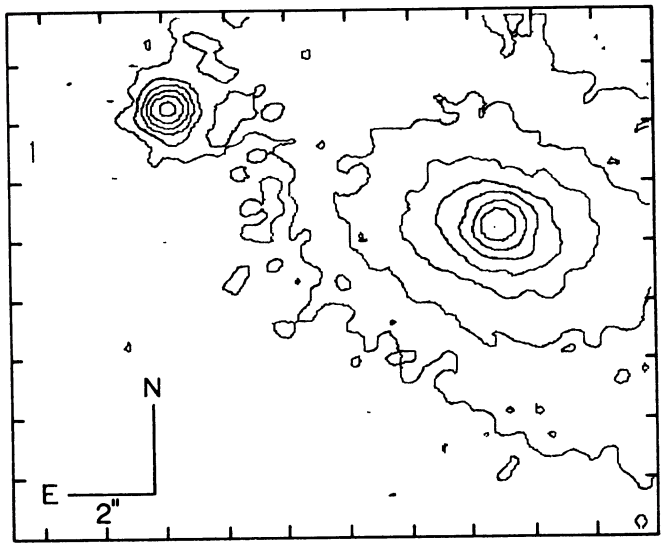


FIG. 3*c*

FIG. 3.—(*a*) Contour plot of the sum of the *J* images with the four quasar components removed, showing the residual galaxy. Also shown are the residual galaxy as it appears in the sum of the (*b*) *H* and (*c*) *K* images. The contour interval and the scale are the same as in Figure 2.

Figure 4 shows that individual components have somewhat different energy distributions as a function of frequency. In particular, components C and D show a steeper decline toward higher frequencies than components A and B. Yee (1988) found that these variations could be explained by selective extinction.

The scale of the gravitational potential of the global mass distribution of the galaxy is so much larger than the size, at the galaxy, of the quasar source that no dependence on source size, and therefore on wavelength, is expected from macrolensing. Microlensing is also unlikely to explain the different energy distributions because, as discussed in § 4, if anything component C is expected to have been amplified with respect to components A and B and amplification by microlensing either should be stronger at higher frequencies or should show very little dependence on frequency.

De Robertis & Yee (1988) obtained spectra of the C III] λ1909 line, redshifted to $\lambda = 5150$ Å, in 1987 November. The line observed in the spectrum of component C has identical equivalent width as that of components A and B, and the flux ratio is similar to that observed by Yee (1988) through the *g* filter (λ4950) at approximately the same epoch. Since the line-emitting region is expected to be much larger than the continuum emitting region in quasars and therefore much less

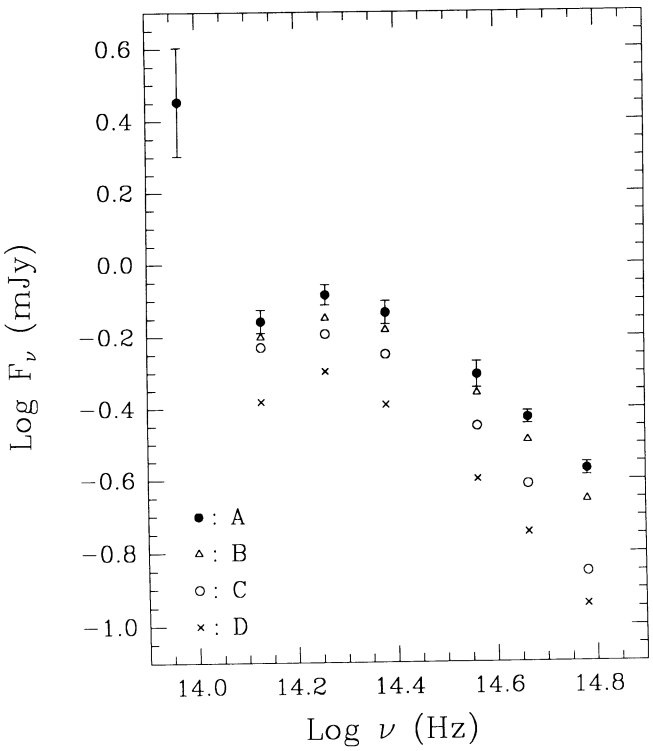


FIG. 4.—Energy distribution of the quasar components in the visible and the near-infrared. The uncertainties for components A, B, and C are similar, while those for component D are higher. The error bars on the 3.3 μm flux of component A do not take into account the uncertainty on the relative [*K* − 3.3] color of the different components.

sensitive to microlensing, this strongly supports the argument that the increasing brightness ratios of components A and B with respect to component C at higher frequencies, shown in Figure 4, are not due to microlensing effects. We conclude that the variation of the brightness ratios with frequency must be due to selective extinction.

The nuclear region of the source was detected through the 3.3 $\mu$m filter on July 21 and July 24. Because the signal-to-noise ratio of the images was low, the brightness of the source at 3.3 $\mu$m obtained on 24 July has been evaluated by comparison with the $K$ band image obtained on the same night. A scaled $K$ band frame was contrasted to the 3.3 $\mu$m frame with an offset between the images of the nuclear region so that their relative brightness could be compared. A scale factor was found by scaling down the $K$ frame until visual comparison of the nuclear images judged them to be of equal brightness. This estimate was made by two independent observers who obtained scale factors of 0.030 and 0.031, respectively; a 20% variation of this scale is adopted as the limit at which one image becomes definitely brighter than the other. From the CFZMs in Table 3, a ratio CFZM($K$)/CFZM(3.3) = 6.34 is adopted, from which the 3.3 $\mu$m flux can be determined.

The scale factor gives the 3.3 $\mu$m strength of the integrated signal from the A, B, C, and D components and the underlying galaxy, in terms of the signal at $K$ from the same components. The color magnitude obtained for this integrated signal is $[K - 3.3] = 1.8$. In order to deduce the 3.3 $\mu$m magnitude of the A component alone, it is necessary to estimate the 3.3 $\mu$m flux from the underlying galaxy and to make the assumption that the $[K - 3.3]$ color magnitude of the four quasar components is the same.

Aperture photometry was done on the galaxy after subtraction of the quasar emission from the $J$, $H$, and $K$ images, and the $g$, $r$, and $i$ images of 1987 September. The energy distributions measured in a 1″ diameter circle, in a 1″–3″ diameter ring, and in a 3″–6″ diameter ring, centered on the nucleus, are plotted in Figure 5. The sky frame subtraction performed on the infrared images was not accurate enough for the direct determination of the emission from the low surface brightness part of the galaxy. The sky level in the infrared images was evaluated by assuming that the flux ratio at 4″ and 11″ from the nucleus along the minor axis of the galaxy was the same in the infrared as in the $r$ band. This could underestimate the sky level if the galaxy becomes redder toward the nucleus. Estimates of the flux were also obtained by using as an upper limit to the sky level the value measured in the infrared images at 11″ from the nucleus along the minor axis. This assumption would lower the calculated fluxes by 8% in the 3″–6″ ring, 3% in the 1″–3″ ring, and 1% in the 1″ circle. Based on this, the systematic uncertainty due to the assumption that there is no color gradient along the minor axis should be no more than a few percent even for the fluxes obtained in the outer ring.

The 1″–3″ ring is where most of the quasar emission is observed. The excellent agreement between the galaxy energy distribution in this ring with that measured in the 3″–6″ ring is an indication of the accuracy of the quasar component subtraction. In all three apertures the energy distribution shows a decrease in the $K$ band after reaching a maximum near the $J$ and $H$ bands. This is typical of the energy distribution observed in spiral galaxies (Sandage, Becklin, & Neugebauer 1969; Frogel 1985), which can be reproduced by synthesis of stellar spectra.

It is therefore justified to assume that the difference in flux between the $K$ and 3.3 $\mu$m bands will follow a Rayleigh-Jeans curve, and that the galaxy contribution to the measured 3.3 $\mu$m emission should be relatively small. The value obtained by assuming that the galaxy and the quasar have the same $[K - 3.3]$ color magnitude should be a conservative lower limit to the 3.3 $\mu$m flux of the quasar components. If the galaxy has $[K - L] = 0.34$, the value obtained for M31 by Sandage et al. (1969), the 3.3 $\mu$m flux from the galaxy should be approximately one-tenth of the total flux from the nuclear region at this wavelength, on the basis of the galaxy and quasar component photometry in the $K$ band. A second comparison was made between the $K$ and 3.3 $\mu$m images with the galaxy contribution to the $K$ image removed, leaving only the signal from the four quasar components. A scale factor of 0.05 ± 0.01 was obtained, again with excellent agreement between the two observers, giving an upper limit to the quasar components flux. A scale factor of 0.045 is adopted to derive the 3.3 $\mu$m flux of component A shown in Figure 4, with the assumption that the four quasar components have the same $[K - 3.3]$ color magnitude.

No matter what the relative $[K - 3.3]$ color magnitudes of the different components are, the observed slope of the quasar spectrum must be steeper from $K$ to 3.3 $\mu$m than in the visible. Neugebauer et al. (1979) have measured a change of the spectral index $\alpha$ ($f_\nu \propto \nu^\alpha$) from $\alpha \approx -0.6$ in the 0.3–1 $\mu$m interval to $\alpha \approx -1.3$ in the 1–3 $\mu$m interval, in the rest frames of the quasars in their sample. A rest wavelength of 1 $\mu$m corresponds to an observed wavelength of 2.7 $\mu$m in the spectrum of the

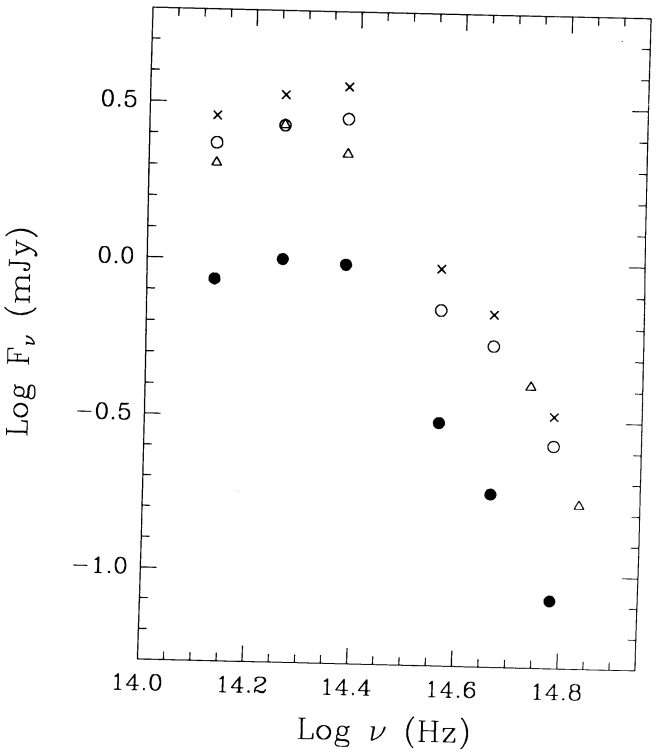


FIG. 5.—Energy distribution of the galaxy after subtraction of the quasar emission. The flux measured within a 1″ diameter circle centered on the nucleus is represented by filled circles, the flux in a 1″–3″ diameter ring by open circles, and the flux in a 3″–6″ diameter ring by crosses (×). The energy distribution observed in NGC 151, an SBbc galaxy, is represented by triangles (Frogel 1985); for ease of comparison the values have been decreased by $\Delta \log F_\nu = 1.0$.

2237+030 quasar components, halfway between the $K$ and 3.3 $\mu$m bands. Assuming that the four components have the same $[K - 3.3]$ color magnitude, a spectral index $\alpha = -3.7$ is obtained between 3.3 $\mu$m and $K$, but an index $\alpha = -1.8$ is obtained between 3.3 $\mu$m and $H$, the difference being due to the dip in the energy distribution observed in the $K$ band. Correction for the reddening between $H$ and 3.3 $\mu$m would make the index somewhat less negative. There is no other example, to our knowledge, of a dip near a rest wavelength of 1 $\mu$m in the published quasar energy distributions. More data are probably needed before an attempt to an explanation can be made. The $H$, $J$, and $i$ fluxes of the A component are well fit by a spectral index $\alpha = -0.65$, while the slope increases at shorter wavelengths presumably due to increased extinction in the intervening galaxy.

The sharp increase of the quasar flux longward of the $K$ band, combined to the decrease of the flux from the galaxy suggests that in the $L$ or the $M$ band it might be possible to find the fifth image of the quasar, predicted by macrolensing models to be nearly coincident with the galaxy nucleus and to have a brightness on the order of a few percent that of component A.

### 3.2. *Light Curve*

Table 5 presents a time history of the measured relative brightness of components B, C, and D with respect to component A. The data are taken from Schneider et al. (1988), Yee (1988), Irwin et al. (1989), Table 4 of this paper, and the $r$ data of 1988 November and 1989 October. The uncertainties assigned to the published data in Table 5 are estimates, based on the uncertainties quoted by the different authors, for the differential magnitudes through the filters used for each observation, except that Schneider et al. (1985) transformed their data to $r$ magnitudes.

The most interesting feature of this table is that the magnitude differences between component A and the other components appear to be larger in 1988 August and September than at the other epochs. In Figure 6, the magnitude difference between components B and A is shown as a function of time. This is the best determined magnitude difference because A and B are the brightest components, they are placed approximately symmetrically with respect to the galaxy nucleus, and they have very nearly the same colors, as shown in Figure 4. The difference in reddening amongst the near-infrared bands is probably negligible compared to the photometric uncertainties. Hence, an average for the $J$, $H$, and $K$ data of $0.13 \pm 0.04$ has been plotted in Figure 6. On the basis of the $g$, $r$, and $i$ data of Yee (1988), the reddening should make (B − A) no more than 0.1 mag higher in $r$ than in the infrared.

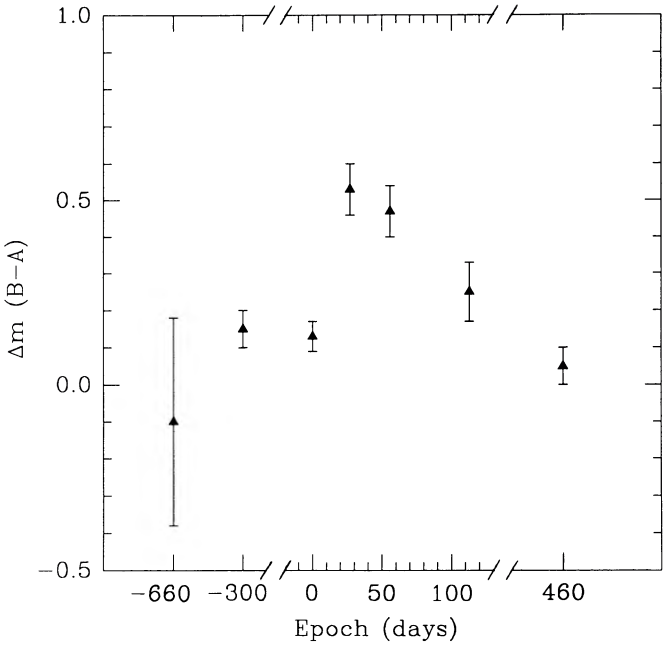


FIG. 6.—Time history of the magnitude difference between components A and B, based on the data of Table 5. The $R$ band data of Schneider et al. (1988) are shown at epoch −660 days, the $r$ band data of Yee (1988) at epoch −300 days, the average of the $J$, $H$, and $K$ band data of 1988 July at epoch 0, the $R$ band data of Irwin et al. (1989) at epochs 27 days and 56 days, and the $r$ band data of 1988 November and 1989 October at epochs 113 days and 460 days, respectively.

## 4. DISCUSSION

### 4.1. *The Extinction Law*

The extinction law has been studied only in our Galaxy and in nearby extragalactic objects (Fitzpatrick 1989). The ability to separate the light from a single source passing through different parts of the interstellar medium of a galaxy offers a

TABLE 5

PHOTOMETRY RELATIVE TO COMPONENT A

| DATE (UT) | FILTER | COMPONENT B | COMPONENT C | COMPONENT D | REFERENCE[a] |
|---|---|---|---|---|---|
| 1986 Sep 28 ..... | $R$ | $-0.10 \pm 0.28$ | $0.33 \pm 0.28$ | $0.83 \pm 0.28$ | 1 |
| 1987 Sep 25 ..... | $g$ | $0.21 \pm 0.05$ | $0.69 \pm 0.07$ | $0.92 \pm 0.08$ | 2 |
| 1987 Sep 25 ..... | $r$ | $0.15 \pm 0.05$ | $0.44 \pm 0.06$ | $0.78 \pm 0.08$ | 2 |
| 1987 Sep 25 ..... | $i$ | $0.13 \pm 0.03$ | $0.36 \pm 0.06$ | $0.73 \pm 0.08$ | 2 |
| 1988 Jul 21–24 ..... | $J$ | $0.12 \pm 0.06$ | $0.29 \pm 0.08$ | $0.65 \pm 0.10$ | 3 |
| 1988 Jul 21–24 ..... | $H$ | $0.17 \pm 0.05$ | $0.27 \pm 0.07$ | $0.54 \pm 0.10$ | 3 |
| 1988 Jul 21–24 ..... | $K$ | $0.11 \pm 0.06$ | $0.18 \pm 0.08$ | $0.56 \pm 0.10$ | 3 |
| 1988 Aug 18 ..... | $R$ | $0.53 \pm 0.07$ | $1.14 \pm 0.07$ | $1.37 \pm 0.07$ | 4 |
| 1988 Sep 16 ..... | $R$ | $0.47 \pm 0.07$ | $0.97 \pm 0.07$ | $1.20 \pm 0.07$ | 4 |
| 1988 Nov 12 ..... | $r$ | $0.25 \pm 0.08$ | $0.63 \pm 0.12$ | $1.00 \pm 0.15$ | 3 |
| 1989 Oct 21 ..... | $r$ | $0.05 \pm 0.05$ | $0.73 \pm 0.08$ | $0.93 \pm 0.08$ | 3 |

[a] (1) Schneider et al. 1988; (2) Yee 1988; (3) This paper; (4) Irwin et al. 1989.

unique opportunity to determine the extinction law for an object located at a distance three orders of magnitude larger than that of any object previously studied.

The flux $f_\lambda$ from quasar component X may be expressed as

$$\log f_\lambda(\mathrm{X}) = \log k_\mathrm{X} + \log f_{\lambda 0} - 0.4 A_\mathrm{X}(\lambda) ,$$

where $f_{\lambda 0}$ is the flux that would be received from the quasar in the absence of extinction and gravitational lensing, $k_\mathrm{X}$ is the lensing amplification factor for component X, and $A_\mathrm{X}(\lambda)$ is the extinction in magnitudes at the wavelength $\lambda$ for component X.

In our Galaxy the extinction laws through the diffuse interstellar medium or the $\rho$ Oph cloud are similar from infrared wavelengths to $\lambda \approx 0.7$ $\mu$m and diverge to an approximate difference of 10% between $\lambda \approx 0.7$ $\mu$m and $\lambda = 4950$ Å (Clayton & Mathis 1988). Considering that the four different quasar components differ in strength at most by 1 mag (at the shortest wavelength), it is reasonable to assume that $A_\mathrm{X}(\lambda) = \alpha_\mathrm{X} A_0(\lambda)$, with a common extinction law $A_0(\lambda)$ for all components. Then the ratio of the fluxes of components X and Y will be given by

$$\log \left( \frac{f_\lambda(\mathrm{X})}{f_\lambda(\mathrm{Y})} \right) = \log \left( \frac{k_\mathrm{X}}{k_\mathrm{Y}} \right) + 0.4(\alpha_\mathrm{Y} - \alpha_\mathrm{X}) A_0(\lambda) .$$

Components A and B have very similar energy distributions, suggesting that the difference between their extinction coefficients is small. The fluxes of components C and D are then compared to those of A and B through the following formulas:

$$\log \left( \frac{f_\lambda(\mathrm{A}) f_\lambda(\mathrm{B})}{f_\lambda^2(\mathrm{C})} \right) = \log \left( \frac{k_\mathrm{A} k_\mathrm{B}}{k_\mathrm{C}^2} \right) + 0.4(2\alpha_\mathrm{C} - \alpha_\mathrm{A} - \alpha_\mathrm{B}) A_0(\lambda) ,$$

$$\log \left( \frac{f_\lambda(\mathrm{A}) f_\lambda(\mathrm{B})}{f_\lambda^2(\mathrm{D})} \right) = \log \left( \frac{k_\mathrm{A} k_\mathrm{B}}{k_\mathrm{D}^2} \right) + 0.4(2\alpha_\mathrm{D} - \alpha_\mathrm{A} - \alpha_\mathrm{B}) A_0(\lambda) .$$

In order to find the ratio $A_0(\lambda)/A_0(V)$ directly from these formulas, it would be necessary to know the amplification ratios $k_\mathrm{A} k_\mathrm{B}/k_\mathrm{C}^2$ and $k_\mathrm{A} k_\mathrm{B}/k_\mathrm{D}^2$. These amplification ratios are uncertain however. Schneider et al. (1988) obtain a macrolensing model for which $k_\mathrm{A} k_\mathrm{B}/k_\mathrm{C}^2 = 1.4$ and $k_\mathrm{A} k_\mathrm{B}/k_\mathrm{D}^2 = 1.6$, but similar models calculated by Kent & Falco (1988) predict $k_\mathrm{A} k_\mathrm{B}/k_\mathrm{C}^2 = 6.0$ and $k_\mathrm{A} k_\mathrm{B}/k_\mathrm{D}^2 = 1.8$.

In the absence of a reliable amplification ratio, it is necessary to assume a value of $A(\lambda)/A(V)$ at some wavelength. Figure 7 shows a comparison between the extinction law in our Galaxy and that obtained from the present data, under the assumption that the extinction ratio $A(K)/A(V) = 0.11$, the value observed in our Galaxy (Clayton & Mathis 1988). The flux ratios of the components at $V$ are determined by interpolation of measured values. The values obtained from the comparison of component C and the comparison of component D with components A and B are averaged together with two times more weight being given to the component C values because of the smaller flux uncertainty and larger extinction coefficient of this component.

The curves for 2237+030 and the Galaxy are seen to be in good agreement. If the extinction in the infrared is indeed only a small fraction of that in the visible in 2237+030, the dust in this galaxy must be dominated by grains of less than 1 $\mu$m in diameter, as in our Galaxy, and the process that determines grain sizes would seem to be quite universal.

The assumption that $A(K)/A(V) = 0.11$ leads to amplification ratios $k_\mathrm{A} k_\mathrm{B}/k_\mathrm{C}^2 = 1.2$ and $k_\mathrm{A} k_\mathrm{B}/k_\mathrm{D}^2 = 2.4$. The ratio for component C is in good agreement with the calculations of Schneider et al. (1988) but differs appreciably from the calculations of Kent & Falco (1988). A higher value of $A(K)/A(V)$ would lead to a lower value of $k_\mathrm{A} k_\mathrm{B}/k_\mathrm{C}^2$. Thus the value predicted by the models of Kent & Falco (1988) cannot be easily explained by extinction. The discrepancy between these models and the ratio observed in the infrared could be explained by strong amplification of component C by microlensing. The good fit between the infrared data obtained in 1988 July and the visible data obtained in 1987 September suggests that the time scale of such a microlensing event would have to be greater than a year.

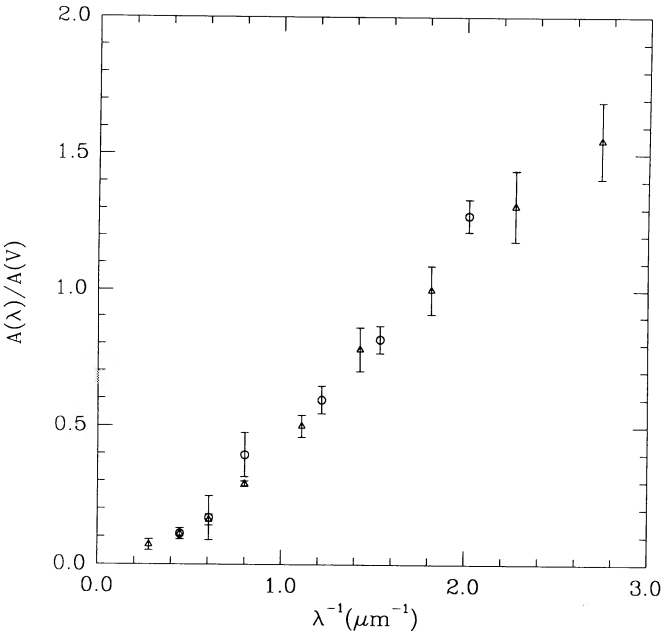


FIG. 7.—Plot of the extinction law as a function of inverse wavelength. The data for diffuse dust in our Galaxy are shown as triangles (Clayton & Mathis 1988), and the data for 2237+030 are shown as circles. The extinction law for 2237+030 was obtained by assuming that $A(K)/A(V) = 0.11$, the value found in our Galaxy. The error bars correspond to the uncertainties on the magnitudes of components C and D relative to A, shown in Table 4.

### 4.2. *Microlensing*

Irwin et al. (1989) have interpreted the brightening of component A that they observed in 1988 August and 1988 September as due to microlensing by an isolated object. On the basis of the data available to them they deduced a maximum duration $\Delta T \sim 420$ days for this event, and they estimated the mass of the lens to be $0.001\ M_\odot < M < 0.1\ M_\odot$, the range of mass being due principally to the unknown tangential velocity of the microlens relative to the line of sight from the observer to the quasar.

To determine whether the infrared data of 1988 July can be used to constrain the time scale of the event observed by Irwin et al. (1989), it is necessary to estimate the expected infrared brightness increase, which may be smaller than the increase observed in the visible because of a larger effective size of the quasar at longer wavelengths.

Malkan (1983) has reproduced the spectra of quasars with optically thick accretion disk models. The accretion disk dominates the emission for $\log \nu_0 > 14.6$, corresponding to $\log \nu > 14.2$ at the redshift of the 2237+030 quasar, while a power-law spectrum dominates at lower frequencies. The tran-

sition region corresponds roughly to the break observed in the energy distribution shown in Figure 4. For a standard optically thick accretion disk around a compact central mass, the dependence on radius of the temperature of the disk surface is $T_S(R) \propto R^{-3/4}$ (Pringle 1981; Novikov & Thorne 1973); this leads to a wavelength dependence of the effective source radius $R \propto \lambda^{4/3}$. From this relation a ratio of 2.3 is obtained between the effective radii at 1.25 $\mu$m ($J$ band) and 0.65 $\mu$m ($R$ band).

The maximum increase in flux due to microlensing, as the source crosses a critical curve, is proportional to $R^{-1/2}$ (Chang & Refsdal 1984), leading to a ratio of 1.5 between the increase in the $R$ band and the $J$ band. This ratio is an upper limit however, and if the source is small compared to the size of the microcaustic, the increase in flux will in fact be slightly greater for a larger source when the source is entirely within the critical curve (see for example Kayser, Refsdal, & Stabell 1986; Wambsganss, Paczyński, & Schneider 1990). Using a ratio of 1.5, a $\sim$30% brightening of component A in the $J$ band should correspond to the 45% increase in the $R$ band reported by Irwin et al. (1989). This would require more than a 3 $\sigma$ deviation from the measured value. It therefore appears that the infrared measurements do constrain the time scale of the microlensing event reported by Irwin et al. (1989).

The infrared data constrain the rise time to $\sim$30 days or less. For any reasonable tangential velocity of the microlens with respect to our line of sight to the quasar this would imply a quasar size of $\sim$1 light-day or less (Irwin et al. 1989). This value is consistent with the size of accretion disks in quasar models (Malkan 1983), and it is significantly smaller than the time scale of the variability of all but a few quasars (Moore & Stockman 1984; Barr & Mushotzky 1986).

The light curve shown in Figure 6 also constrains the duration of the event to $\Delta T \sim 100$ days. Since $\Delta T \propto M^{1/2}$ for microlensing by a single object, this shorter time scale applied to the Irwin et al. (1989) model would imply that the microlens had a mass $0.0006\,M_\odot < M < 0.006\,M_\odot$, and this could be the first evidence of the existence of a substellar mass outside our Galaxy or even outside the solar system.

It must be emphasized, however, that this mass estimate is valid only if the event observed in 1988 did correspond to the passage of the source into and out of a single microcaustic. If the optical depth to microlensing is high, a line of sight through the galaxy is likely to encounter more than a single microcaustic. An amplification event then corresponds to the passage of the source through a single critical curve. The duration of the event may still be used to estimate the size of the source, but not the size of the microcaustic (or the mass of the microlens).

It is as yet uncertain whether isolated microcaustics are likely to occur in 2237+030. Wambsganss, Paczyński, & Katz (1990) and Wambsganss, Paczyński, & Schneider (1990) have calculated the effects of microlensing in 2237+030. These calculations show that if the surface mass density obtained from the macrolensing models is dominated by stars, the optical depth to microlensing should be high. Inspection of Figure 1 of Wambsganss, Paczyński & Schneider (1990) suggests that a decrease of the estimated star density by a factor of $\sim$3 would make isolated events a likely occurrence. A lower estimate of the star density would be justified if, (1) a massive central object accounts for a good part of the macrolensing effect (Schneider et al. 1988), or (2) a large fraction of the mass density is in the form of interstellar gas. The density of interstellar molecular gas increases sharply towards the center of spiral galaxies; in our Galaxy it accounts for approximately half of the mass within 500 pc of the center (Faber & Gallagher 1979; Scoville & Sanders 1987).

## 5. SUMMARY

This paper has presented infrared and visible photometry of the 2237+030 lensed quasar emission, from which the following results were obtained:

1. The energy distribution of the quasar components shows evidence of differential extinction between the different components. An extinction law has been deduced with the assumption that $A(K)/A(V)$ has the same value as in our Galaxy. Using a Hubble constant $H_0 = 75$ km s$^{-1}$ Mpc$^{-1}$, the distance to the galaxy is 160 Mpc, orders of magnitude father away than any other object for which an extinction law has been obtained. Further observations of 2237+030 in the $K$, $L$, and $M$ bands could determine the zero point of the extinction law.

2. The energy distribution of the quasar has a minimum in the $K$ band and shows a large increase at 3.3 $\mu$m. The change in slope near a rest wavelength of 1 $\mu$m is qualitatively similar to that observed in other quasars, but the dip in the $K$ band has not been reported for any other quasar.

3. The data presented in this paper constrain the rise time and the duration of the microlensing event reported by Irwin et al. (1989). The rise time implies that the size of the quasar continuum source is of the order of 1 light-day or less. If the 1988 event can be shown to be caused by a single isolated body, the duration of the event implies a substellar mass for the microlens.

Monitoring the brightness variations of the quasar components in the infrared and the visible during microlensing events will make it possible to determine the source size as a function of wavelength and to test quasar models. This will require systematic photometric observing over several years.

The authors would like to thank the staff of the Canada-France-Hawaii Telescope, in particular Bill Cruise, Ken Barton, and John Hamilton, for their assistance with the observations. The infrared observations would not have been possible without the strong support of the director, Robert McLaren, whom we gratefully thank. We also thank H. Grondines and M. Riopel for help with the data reduction, and M. Langlois for the artwork. D. N. and H. C. K. Y. are supported through the Natural Science and Engineering Research Council by University Research Fellowships and operating grants. W. J. F., J. D. G., Z. N., and J. L. P. were supported by grants from the NSF, NASA-Ames, the National Geographic Society, and NASA.

## REFERENCES

Barr, P., & Mushotzky, R. F. 1986, Nature, 320, 421
Blackwell, D. E., Leggett, S. K., Petford, A. D., Mountain, C. M., & Selby, M. J. 1983, MNRAS, 205, 897
Chang, K., & Refsdal, S. 1984, A&A, 132, 168
Clayton, G. C., & Mathis, J. S. 1988, ApJ, 327, 911
De Robertis, M. M., & Yee, H. K. C. 1988, ApJ, 332, L49
Epchtein, N., Braz, M. A., & Sèvre, F. 1984, A&A, 140, 67
Faber, S. M., & Gallagher, J. S. 1979, ARA&A, 17, 135
Filippenko, A. V. 1989, ApJ, 338, L49
Fitzpatrick, E. L. 1989, in IAU Symposium 135, Interstellar Dust, ed. L. J. Allamandola & A. G. G. M. Tielens (Dordrecht: Kluwer), p. 37
Forrest, W. J., Pipher, J. L., Ninkov, Z., & Garnett, J. D. 1989, in Proc. of the 1989 Infrared Detector Tech. Workshop, ed. C. R. McCreight (NASA Tech. Memo. 102209), p. 157

Frogel, J. A. 1985, ApJ, 298, 528
Gehrz, R. D., Hackwell, J. A., & Jones, T. W. 1974, ApJ, 191, 675
Gillett, F. C., Merrill, K. M., & Stein, W. A. 1971, ApJ, 164, 83
Gunn, J. E., & Oke, J. B. 1975, ApJ, 195, 255
Huchra, J., Gorenstein, M., Kent, S., Shapiro, I., Smith, G., Horine, E., & Perley, R. 1985, AJ, 90, 691
Irwin, M. J., Webster, R. L., Hewett, P. C., Corrigan, R. T., & Jedrzejewski, R. I. 1989, AJ, 98, 1989
Kayser, R., Refsdal, S., & Stabell, R. 1986, A&A, 166, 36
Kayser, R., Refsdal, S., Stabell, R., & Grieger, B. 1987, in IAU Symposium 124, Observational Cosmology, ed. A. Hewitt, G. Burbidge, & L. Z. Fang (Dordrecht: Kluwer), p. 767
Kent, S. M., & Falco, E. E. 1988, AJ, 96, 1570
Malkan, M. A. 1983, ApJ, 268, 582
Moore, R. L., & Stockman, H. S. 1984, ApJ, 279, 465
Neugebauer, G., Oke, J. B., Becklin, E. E., & Matthews, K. 1979, ApJ, 230, 79
Novikov, I. D., & Thorne, K. S. 1973, in Black Holes, ed. C. DeWitt & B. DeWitt (New York: Gordon & Breach), p. 343
Oke, J. B., & Schild, R. E. 1970, ApJ, 161, 1015
Paczyński, B. 1986, ApJ, 301, 503
Pringle, J. E. 1981, ARA&A, 19, 137
Sandage, A. R., Becklin, E. E., & Neugebauer, G. 1969, ApJ, 157, 55
Schneider, D. P., Turner, E. L., Gunn, J. E., Hewitt, J. N., Schmidt, M., & Lawrence, C. R. 1988, AJ, 95, 1619
Scoville, N. Z., & Sanders, D. B. 1987, in Interstellar Processes, ed. D. J. Hollenbach & H. A. Thronson (Dordrecht: Kluwer), p. 21
Tyson, J. A. 1986, in IAU Symposium 119, Quasars, ed. G. Swarup & V. K. Kapahi (Dordrecht: Reidel), p. 551
Wambsganss, J., Paczyński, B., & Katz, N. 1990, ApJ, 352, 407
Wambsganss, J., Paczyński, B., & Schneider, P. 1990, ApJ, 358, L33
Yee, H. K. C. 1983, ApJ, 272, 473
———. 1988, AJ, 95, 1331
———. 1991, PASP, submitted